This pre-print is under review at the journal *Frontiers in Earth Sciences* and is deposited on the EarthArXiv platform.

Pleistocene coastal evolution of the Makran subduction zone

By

Raphaël Normand[1](raphnormand@gmail.com), Guy Simpson[1](guy.simpson@unige.ch) and Abbas Bahroudi[2](bahroudi@ut.ac.ir)

1 Department of Earth Sciences, University of Geneva, Rue des Maraîchers 13, CH-1205 Genève.
2 Exploration department, School of Mining Engineering, University of Tehran, Northern Kargar avn, P.O. Box 11365-4563,Tehran, Iran.

Pleistocene coastal evolution of the Makran subduction zone

Raphaël Normand1*, Guy Simpson1 and Abbas Bahroudi2

[1]Department of Earth Sciences, University of Geneva, Rue des Maraîchers 13, CH-1205 Geneva.
[2]Exploration Department, School of Mining Engineering, University of Tehran, Northern Kargar avn, P.O. Box 11365-4563, Tehran, Iran.

*** Correspondence:**
Raphaël Normand
raphnormand@gmail.com

Makran subduction zone, Marine terrace deposits, Coastal evolution, Differential erosion, Uplifted beach, Headland bay beach

Abstract

Along the coast of the Makran subduction zone (SE Iran and SW Pakistan), active uplift combined with efficient erosion and vigorous sediment transport have led to marine terraces with unique morphology and sedimentology. These terraces are characterized by the systematic presence of an extensive 1-10+m thick sandstone layer capping their wave-cut base. Our investigation of thirty-six sedimentary logs of the terrace deposits revealed a general prograding trend from nearshore to beach deposits moving upsection. The presence of a thick marine sedimentary succession above the erosive platform suggests continued creation of accommodation space following carving of the platform by wave-erosion (i.e., erosion of the platform occurred before the peak of the highstand). Deposition of prograding beaches above the platform is interpreted to have occurred during the sea-level stillstand and the start of sea-level fall and was favoured by a high sedimentary supply. While some terraces evolve into a classic staircase morphology, others are found as flat-topped platforms bounded by steep cliffs, isolated within the low-lying coastal plain. We find that this morphological difference results from a contrast in bedrock erodability (resistant sandstone versus soft marl, respectively). The flat-topped isolated marine terraces with marl bedrock share morphological and sedimentological similarities with Holocene crenulated beaches currently developing in low-lying bays between headlands. As indurated beaches are uplifted into headlands, they influence the development of following generations of beaches before being eroded by surficial erosion and wave action. Our study shows that the coastal geomorphology of the Makran coast is dictated by the interaction between tectonics (providing relative sea-level fall and juxtaposing units of different erodability at the same structural level by faulting), differential erosion between hard and soft rock (responsible for the presence of isolated headlands) and coastal sedimentary transport processes (permitting accumulation of extensive beach deposits).

1. Introduction

The Makran subduction zone (MSZ) is an ideal natural laboratory to study coupled interactions between active sedimentation, erosion and tectonics. This is due to the combined effects of several competing factors. First, the region is arid and sparsely vegetated, making its geology exceptionally well exposed. Second, the margin is experiencing rapid surface uplift, linked to subduction of the oceanic portion of the Arabian plate beneath the continental Eurasian plate. Third, the subduction zone experiences a high sedimentary input from subaerial portions of the eroding accretionary prism.

Here we have studied a series of peculiar uplifted marine terrace deposits that reflect these competing phenomena. These terraces are somewhat unusual because they are both erosional and depositional, i.e., they form in response to widespread marine erosion during sea-level highstands, but they are covered with often thick veneers of shallow marine sediment (hereafter referred to as "terrace deposits") that reflect the high sediment input into the coastal region. These terraces are distinctly different from most other marine terraces that are dominantly erosive (e.g., Lajoie, 1986; Anderson et al., 1999). The Makran marine terraces (Mmt) are also intriguing because their preservation and evolution depends sensitively on the nature (erodability) of the local bedrock (i.e., sandstone versus marl).

In this study, we have investigated the morphology and sedimentology of the Makran marine terraces using a combination of satellite imagery, DEM analysis, and fieldwork. In another recent study, we have constrained the ages of the terraces using C14, U-Th series and OSL dating (Normand et al., 2019b). Here we attempt to answer the following questions: What does terrace deposit sedimentology tell us about the coastal setting during previous highstands? Why are the terraces found as isolated platforms or headlands and what controls their distribution along the coast? Which marine terrace definition best suits the Makran marine terraces? How did the Makran coast evolve throughout the Late Pleistocene? Ultimately, our study aims to improve our general understanding of interactions between tectonic uplift, eustasy, surface processes and coastal sedimentation.

2. Geological setting

The area studied sits on the coastal margin in the upper plate of the Makran subduction zone (MSZ), located in southeastern Iran. At this margin, the oceanic Arabian plate is currently passing northwards beneath the continental Eurasian plate at a rate of approximately 2 cm/y (e.g., Vernant et al., 2004; Masson et al., 2007; Khan et al., 2008; Frohling and Szeliga, 2016). Although the MSZ has low historical seismic activity, especially the western segment (Byrne et al., 1992), tectonic uplift of the prism is evidenced by the presence of numerous marine terraces along the coast (Fig. 1) (e.g., Page et al., 1979; Snead, 1993; Normand et al., 2019). The thick pile of emerging sediments comprising the prism are Himalaya derived (Harms et al., 1984). However, most sediments on the modern coast are reworked from emerged portions of the accretionary prism residing to the north of the studied area (McCall and Kidd, 1982; Ellouz-Zimmermann et al., 2007; Bourget et al., 2010).

The Makran area presently has an arid climate with a low yearly mean precipitation (~97-127 mm at the coastline (Sanlaville et al., 1991)) and sparse vegetation cover. Rain events are rare but intense, occurring mainly in winter. These events induce substantial erosion of the soft sedimentary rocks of the prism, river re-activation and flooding of the coastal plain. The tidal range is micro to mesotidal (1.8-2.7m (Snead, 1993)). In the western Makran, waves and wind come mainly from the SSE (Saket and Etemad-shahidi, 2012).

2.1 Geology at the coastal Makran

The pre-Quaternary bedrock of the coastal margin in the eastern Iranian Makran consists of sedimentary rocks of Upper Miocene to Pliocene age (Samadian et al., 1994; Samadian et al., 1996; Samadian et al., 2004) (Fig. 2). Although these units have formation names in the Pakistani Makran (e.g., Ormara, Chatti, Talar formations (Harms et al., 1984)), correlation with the unnamed formations of the Iranian Makran has not yet been established. The three broad Tertiary units relevant to this paper can be differentiated on the basis of their lithology and age (Fig. 2). The base and top of the sequence is made of two formations of Upper Miocene and Pliocene age, respectively (Samadian et al., 1994; Samadian et al., 1996; Samadian et al., 2004), with a sandstone-dominated lithology. These typically consist of an alternance of sandstones and finer marly layers, that are associated with regression and transgression of the coastline on shallow wave-dominated shelves (Harms et al., 1984). The middle interval (Upper Miocene) is composed of fine-grained slope marl deposits occasionally intercalated with thin sandstone layers (Harms et al., 1984) and incorporating pipes or boudins of orange mudrock (that we suspect are derived from mud volcano activity) as well as gypsum veins (Normand et al., 2019a, Figs. M).

These Tertiary sedimentary units are faulted and deformed into wide, gently double-plunging, E-W trending anticlines and synclines, visible in satellite imagery (Farhoudi and Karig, 1977; Leggett and Platt, 1984; Samadian et al., 1994; Samadian et al., 1996; Samadian et al., 2004) (Fig. 2). Although reverse faulting is associated with the growth of folds both in the immerged part of the prism (offshore) and north of the coastal region (White and Louden, 1982; Grando and McClay, 2007), normal faults predominate close to the coastline (Ghorashi, 1978; Harms et al., 1984; Platt and Leggett, 1986; Snead, 1993; Dolati and Burg, 2012).

The topography of the coastal area is mostly dominated by a flat and wide (about 20km) coastal plain, which contrasts with the rugged morphologies of both the Makran ranges (the name given to the mountains extending north of the coastal plain) and the coastal headlands hosting Quaternary marine terraces (Fig. 1b). Although the coastal plain is mostly covered by a thin veneer of modern fine-grained distal alluvial fan deposits, a few outcrops reveal the nature of the underlying bedrock, which consists predominantly of Upper Miocene grey marls. These rocks are often deeply eroded (forming badland topography), except where they are preserved under layers or debris of indurated Quaternary deposits (marine terraces or fluvial terrace deposits) (Normand et al., 2019a, Figs. M, GU, PA, TA).

Numerous normal faults are observed to cut the sediments of the Makran coastal area. These faults strike dominantly parallel to the coast and dip towards the south (or less commonly the north). Faults have throws ranging from less than a meter to more than fifty meters. These faults are important for the development and preservation of marine terraces in the region because they can juxtapose units of drastically different erodability to the same structural level (Fig. 3). For example, in the vicinity of Chabahar, a series of large headland bounding normal faults have locally juxtaposed easily erodable Upper Miocene marls against relatively resistant Pliocene sandstones (Fig. 3). This results in topographic inversion whereby the downthrown block stands high because it is more resistant than the adjacent upthrown marl block (Fig.3). Normal motion on these faults is confirmed by local drag features, Riedel shears and terrace offsets (Normand et al., 2019b; Normand et al., 2019a). Note that although the relative motion between the headland and the coastal plain is due to normal faulting, the general regional trend remains uplift, as attested by the presence of marine terraces on the downfaulted headland. Only the Chabahar headland was directly observed to be bound by normal faults. However, the Tang and Konarak headlands of Tertiary sandstones also show sharp boundaries with the coastal plain, which might also suggest the presence of faults controlling the limits of these headlands (Fig. 2).

Along the seaward margin of the coastal plain, two types of protruding headlands are found. While the firsts are these localized outcrops of sandstone-dominated bedrock, the seconds are high, flat platforms, characterized by a planar layer of marine terrace deposits capping grey marl bedrock (more details in section 4.1). Between the protruding headlands, the coastline has developed into deep bays hosting extensive successions of beach ridges (Fig. 1), deposited since the Holocene maximum transgression (Gharibreza, 2016; Shah-Hosseini et al., 2018).

3. Marine terraces: General definitions

Marine terraces are geomorphic features found along coastlines subject to relative sea-level changes (Lajoie, 1986). Marine terraces can be divided into three broad categories: constructional, erosional and depositional terraces. Constructional terraces are formed mainly by coral reef development and are not considered further here since the Makran coast rarely hosts coral constructions.

Erosional wave-cut platforms are planar surfaces incised by wave action into the underlying bedrock. Through the combined effects of eustatism and tectonics, these surfaces may be emerged, after which time they start to degrade by weathering and erosion while younger surfaces develop in a lower position (Anderson et al., 1999). Because the erosive energy available at the base of a sea cliff is reduced as the wave power dissipates across an expanding platform, the development of platforms becomes increasingly difficult as they widen. Modelling has shown that amongst parameters controlling platform width, there is the strength (resistance) of the bedrock, the presence of debris protecting the cliff foot, the tidal range and the duration of the sea-level stillstand (e.g., Anderson et al., 1999; Trenhaile, 2000; Trenhaile, 2002). Moreover, because younger terraces develop at the expense of older ones, some terrace levels might be entirely erased from the geomorphic record. Computer models of shore development have shown that erosion is more effective during episodes of relative sea-level rise than fall (e.g., Trenhaile, 2002). However, studies of modern cliff retreat rates by cosmogenic nuclides tend to indicate steady or even increasing coastal retreat rates since the mid-Holocene highstand (Regard et al., 2012; Hurst et al., 2016).

The term wave-built terrace has been used to describe a variety of different coastal landforms, without a clear definition (Dietz, 1963). The term was originally defined by Gilbert (1890) to describe paleobeach ridge successions on Lake Bonneville. It was subsequently traditionally re-used to characterize subaqueous platforms, created by sedimentary accumulation at the seawards edge of a wave-cut platform (Dietz, 1963; Bird, 2000). The latter, observed in modern coastline settings, are rarely preserved in the fossil record (Dietz, 1963). Following the original idea of Gilbert (1890), Jara-Muñoz and Melnick (2015) have defined wave-built marine terraces as stacked patterns of sediments deposited above a wave-cut platform. The difference with a wave-cut platform covered by sediments is that the sedimentary succession of a wave-built terrace has a certain degree of complexity in its sedimentary succession.

4. The Makran marine terraces

Along the Makran coast, the Tertiary basement units are commonly overlain by extensive marine terraces. These terraces are typically characterized by a 1-10 m thick shelly sandstone deposits that cap the underlying basement sediments along a wave-cut unconformity (Falcon, 1947; Little, 1972; Page et al., 1979; Snead, 1993). The sedimentary succession of the terrace deposits has been described as beach deposits (Falcon, 1947; Vita-Finzi, 1980; Snead, 1993), though only a few detailed sections have been previously described (Little, 1972; Normand et al., 2019b). Some authors

have argued that a few terraces, showing sharp linear edges parallel to the coastline (e.g., Konarak, Gurdim), might have developed on horsts (Little, 1972; Snead, 1993).

The necessity of widespread and accurate dating of the Mmt in order to derive surface uplift rates has been pointed out by Vita-Finzi (1980). Most previous dating attempts on the Mmt were done by radiocarbon dating of shells sampled within the terrace deposits, which yielded ages greater than 20 ka, interpreted as minimum ages (Vita-Finzi, 1975; Page et al., 1979; Vita-Finzi, 1980; Vita-Finzi, 1981; Reyss et al., 1998; Rajendran et al., 2013; Haghipour et al., 2014). Recently, OSL dating of the Iranian (western) Makran terraces has permitted the correlation of the marine terrace sequences to past sea-level highstands. The results revealed that most marine terraces formed between MIS5 and MIS 17, with two very young surfaces dated at MIS3 (Normand et al., 2019b). Calculation of uplift rates revealed moderate to high uplift rates along the Iranian Makran coast (0.05 - 1.5 mm y^{-1}), with an exceptionally high and variable uplift rate in Pasabander area, close to the border with Pakistan (1 - 5 mm y^{-1}) (Normand et al., 2019b). Dating of the marine terraces is not the focus of this paper, though knowledge of their age is important, especially from a geomorphological point of view.

4.1 Terrace morphology

Our study of the Makran marine terraces revealed two distinctive terrace morphologies, based on the nature of the bedrock into which the terrace was carved (indurated sandstone-dominated lithology versus erodible marl-dominated lithology). Terraces built on sandstone-dominated headlands (hereafter referred to as sandstone-type terraces) have a classic staircase morphology that reflects recent trends of relative sea-level change (Fig. 4a) (Lajoie, 1986; Anderson et al., 1999; Trenhaile, 2002). Sequences of such terraces are relatively extensive, with 6+ levels in Chabahar, possibly ranging back to MIS 17 (Normand et al., 2019b). Each terrace is generally backed by a paleocliff (that can be topped by an older terrace) at the base of which fossil rockfall megaboulders are sometimes found embedded within the terrace deposits (Fig. 4b) (Normand et al., 2019b). While the bedrock bedding is most of the time tilted owing to prism deformation (e.g., Fig 4b), subhorizontal resistant Tertiary sandstone beds sometimes closely resemble marine terraces (Snead, 1993).

Terraces built on marl-dominated bedrock (hereafter referred to as marl-type terraces) have a singular morphology. They are wide platforms (up to 5 km) bounded by steep cliffs carved within the marl bedrock and capped by terrace deposits (Fig. 4c). Most of the time, the paleocliff backing the terrace is degraded into badlands or eroded down to the level of the coastal plain (Fig. 4c, 4d). Where the layer of the terrace deposit is breached, the marl bedrock is heavily eroded into steep marl cliffs (Fig. 4d). Sequences of such terraces comprises up to four levels, the upper levels being highly degraded into isolated platforms less than a square kilometer in area. Dating results from marl-type terraces show relatively young ages, with some terraces attributed to MIS 3 (e.g., in Pasabander region) and potentially going back to maximum MIS 5e, for the most degraded surfaces (Normand et al., 2019b).

Some terraces (mostly marl-type) have peculiar curved borders, not parallel to the general trend of the modern coastline. This curved morphology is also expressed and accentuated by lineations visible in satellite imagery on terrace surfaces (Fig. 4c, see also Fig. 8g). Field investigation of the linear markers revealed that they are the morphological expression of the top of the terrace deposits composed of gently sloping (nearly horizontal) sandstone sedimentary structures (Normand et al., 2019a, Figs. PA5-6). Another geomorphological characteristic of these terraces is their peculiar "finger-like" protrusions (Fig. 4c). This morphology, defined by Little (1972), is caused by stream erosion following the main dip of the terrace surface.

4.2 Terrace sedimentology

All Iranian (and seemingly Pakistani (Snead, 1967; Snead, 1993)) Mmt share a common characteristic: They are capped by a layer of marine sediments of thickness varying between 1 and 10 meters (possibly thicker in the eastern Makran) (Fig. 4e). Thirty six sections into the Iranian marine terrace deposits were logged in order to understand the processes responsible for the deposition of these layers (supplementary data III, table A). Localities were chosen based on their accessibility, but also with the objective of collecting information from the back of the terrace (at the base of the paleocliff) (SA, ESA), the middle (MT) and the seawards edge (SS) of the terrace, to understand lateral variability in the sedimentology (Fig. 6a and its caption). We divide the sedimentary logs into broad facies (Table 1), based on grain-size and sedimentary structures, while the vertical relationships between facies are reported in Figure 6a (Fig. 5 contains the logs legends).

Makran terrace deposits follow the same general sedimentological trend. The transition between Tertiary bedrock and marine terrace deposits is an erosive surface, most of the time evidenced by an angular unconformity (e.g., Fig. 4a, 4b). Direct access to the full extent of the erosive surface is prevented by the presence of the terrace deposits, though flatness and continuity of this surface can be estimated from natural sections provided at the terraces' borders. Recurrently, the base of the terrace deposits incorporates sandstone boulders and pebbles (~5-50 cm diameter, some of which are bored by lithophaga mollusks) embedded within the overlaying deposit (Fig. 4e, Fig. 6a). At the back of those terraces backed by a paleocliff, megaboulders (rockfall, of 0.5 to 3m+ diameter) are found embedded into the terrace deposits (Fig. 4b) (Normand et al., 2019a). Forming the main body of the terrace deposits, sandy material and shell fragments are arranged into sedimentary structures, such as trough cross stratification (usually at the base of the deposits) and horizontal laminations (usually topping the section) (Table 1) (e.g., Fig. 4e). Some sections, situated close to river mouths, incorporate conglomerate layers. We report the possible occurrences of erosive surface within the stratigraphy of the terrace deposits, although these are difficult to ascertain (Fig 6a, section R9, R10).

4.3 Depositional facies interpretation

The type of sediments comprising the terrace deposits are independent of their bedrock type. The presence of boulders and pebbles at the base of many logs, is interpreted as lag deposits associated with the transgressive ravinement surface (i.e., the wave-cut platform) (Catuneanu et al., 2011). The recurring occurrence of megaboulders embedded at the back of some terraces implies a certain degree of cliff foot protection as sedimentation starts. The lower sandy units incorporating trough cross-stratifications or other evidences of energetic currents are interpreted as shoreface deposits, whereas the overlying sandy laminated facies is interpreted to be deposited in the swash zone (Table 1) (e.g., Tamura, 2012). Eolian deposits are rarely preserved (only in log K1). In summary, the general trend is progradational, with all logs evolving from shoreface at the base to foreshore at the top (Fig. 6).

While the general shallowing upwards trend described above is true for all logged transects, some incorporate other sedimentological complexities. Conglomerate layers within some terrace deposits (intercalated with shoreface facies) (Fig. 6a) are interpreted as mouth bar deposits (related to river discharge). A fine-grained, nonlaminated facies is observed at the base of some logs, just above the wave-cut platform. This indicates the presence of lagoonal systems at the coastline during the early stages of the highstand. Similar observations were made from Holocene successions in the Makran, where early Holocene (8ka-6ka) lagoonal deposits are found at the base of post mid-Holocene highstand sandy beach successions (Sanlaville et al., 1991). Erosive surfaces within logs of Ramin T1 (R9, R10) are related to episodes of re-occupation of the lower, seawards parts of the platform (Jara-Muñoz and Melnick, 2015).

5. Discussion

5.1 Depositional model

Observations of the terrace deposits led us to the following depositional model (Fig. 7). Carving of the platform seems to have occurred during the early stages of the sea-level highstand (associated with sea-level rise) and carried on until wave-energy was insufficient to further extend the platform (Anderson et al., 1999; Trenhaile, 2002) (Fig. 7a). Platform width being partially controlled by the erodability of the bedrock, marl-type terraces are usually wider than sandstone-type terraces. The thickness of the terrace deposits (up to 10 m, even at the back of the terrace, Fig. 6a) attests the continued creation of accommodation space following the carving of the shoreline angle. Hence, we suggest that most of platform erosion occurs during sea-level rise and the first sedimentary layers, deposited near the shoreline angle and above the wave-cut surface, should be aggradational (Fig. 7b). The middle to late stages of the highstand are dominated by shallowing-upward sedimentation, as prograding beaches develop above the wave-cut surface due to relative sea-level fall and the high sedimentary input along the Makran coast (Fig. 6a, Fig. 7c, 7e). This last event differentiates the Mmt from most marine terraces in other parts of the world, which are usually either uncovered, or capped by only a thin veneer of colluvium (with some exceptions (Dupré, 1984; Jara-Muñoz and Melnick, 2015)).

There are several sedimentological and morphological parallels between modern bay beaches and the deposits of the marl-type terraces (Fig. 8). For example, both comprise prograding, shallowing upward sequences (Page et al., 1979; Vita-Finzi, 1980; Sanlaville et al., 1991; Haghipour et al., 2014; Gharibreza, 2016; Shah-Hosseini et al., 2018), although, the Holocene beach sequences contain much more fine-grained (lagoonal) deposits than the older terrace deposits (Sanlaville et al., 1991). The curved shaped terraces with finger-like morphologies closely resemble the Holocene crenulated bay beaches that develop in the sections of the coastline with erodible marl bedrock (Fig. 8e-8h) (Yasso, 1965; Valvo et al., 2006; Limber et al., 2014; Hurst et al., 2015). Parallel curved lineations observed on the surface of the terraces in satellite imagery are the surficial expression of gently sloping swash planar laminations within the terrace deposits (Normand et al., 2019a, Fig. PA5-6). These are therefore, the equivalent of modern beach ridges. Moreover, most of the time, the curved lineations on marine terraces are associated with a paleo-headland in the form of a higher terrace, or a sandstone bedrock outcrop (e.g., Tang terraces; Fig. 8e, 8f, Pasabander T2 and T3; Fig. 8g, 8h). Hence, the peculiar isolated marl-type terraces are the uplifted and degraded equivalent of modern bay-beaches (see section 5.3) (Fig. 7e-7f). During the early stages of a highstand, a wide and shallow platform is carved into the marl bedrock. Owing to high sedimentation, relative sea-level fall and the small accommodation space available, beach progradation above the platform is fast (Fig. 7e) (Gharibreza, 2016; Shah-Hosseini et al., 2018).

In summary, we believe that the Mmt are carved by wave-cut incision during the early stages of a sea-level highstand, as the sea re-occupies the coastal area. At the maximum transgression and during the relative sea-level fall that follows, coverage of the platform by prograding marine coastal sedimentation, such as beach, lagoonal and other nearshore deposits is favored by the long-term uplift of the coast and the active sedimentary environment of the coastal MSZ (Fig. 7).

5.2 Characterization of the Makran marine terraces

Although the marl and sandstone-type terraces exhibit different geomorphological aspects, all Mmt are composed of a wave-cut surface above which a prograding beach sedimentary succession is deposited. In this respect, they cannot be defined as pure wave-cut terraces. As seen in section 3, the

term wave-built marine terraces has been used to describe several different coastal landforms, not always corresponding to the Mmt. However, the marl-type terraces share exactly the same structures that inspired the original definition of Gilbert (1890), that is; prograding beach ridges deposited above a wave-cut surface.

According to Jara-Muñoz and Melnick (2015), wave-built marine terraces are stacked patterns of sediments deposited above a wave-cut platform. They also suggest that headlands (exposed to wave attack) are more prone to develop into wave-cut terraces, while embayments (favoring sediment accumulation) would host wave-built terraces. The Mmt fit this definition and support these suggestions; although headland (sandstone-type) terraces of the Makran also include a stacked pattern of sediments above their wave-cut surface (a characteristic of all Makran terraces), it is manifest that marl-type terraces used to be relatively more extensive and had well developed beaches compared to their headland counterparts.

5.3 Differential erosion

In the Makran, differential erosion between resistant sandstone and soft marl is a key factor in shaping of the current coastal geomorphology. The topography at the coastline is a direct reflection of the distribution of bedrock lithology, which is itself strongly influenced by local downfaulting of Pliocene blocks. Relief along the Makran coast are dominated by resistant sandstones, whereas the coastal plain with marl-dominated bedrock is leveled to the base level corresponding to rivers longitudinal profiles (unless protected by a resistant layer) (Fig. 1b). A prime example of differential erosion is the Chabahar headland. As reported in this study, the headland is bordered by normal faults and therefore is a downfaulted block. However, counter intuitively, the footwall is eroded, whereas the hanging wall is preserved (Fig. 3).

When erosion is significant, a distinction needs to be made between rock uplift rates and surface uplift rates (England and Molnar, 1990). While the first is the uplift rate of a rock body relative to a fixed point (e.g., due to tectonic forces), the second corresponds to uplift of Earth's surface and as such, considers erosion as a factor counteracting uplifting forces. Terraces sediments of the Makran were deposited close to sea level; they can therefore be used as markers for relative sea level change. While a solidified beach is resistant to erosion, the erodible nature of the paleo coastal plain has contributed, together with tectonic uplift, to create a topographic anomaly below the marine terrace deposits by differential erosion (Fig. 7e, 7f). Surface uplift rates below the capping deposits is equivalent to rock uplift, as the erosion rate of the solidified beach deposit is close to zero. However, in the coastal plain, erosive forces have completely counterbalanced rock (tectonic) uplift rates, implying surface uplift rates close to zero (Fig. 9). In fact, we can infer marl erosion rates by knowing rock uplift rates from the dating results on the marine terraces (Normand et al., 2019b).

One of the best illustrations of these effects is seen in the Pasabander area. In this region, breached terraces with marl bedrock are efficiently eroded down to base level leaving isolated terrace remnants overlooking the coastal plain, bounded by vertical cliffs on both the seaward and landward sides (Fig. 4d, Fig. 8g, Fig. 10b). In this regard, it is understandable why there is such a difference in grain size between the Holocene coastal deposits, incorporating substantial fine grained lagoonal material, and the terrace deposits of mostly sandy facies; the fine-grained, lagoonal portion of terrace deposits has a low preservation potential and was probably eroded. Moreover, non-indurated sandy facies (such as dry eolian facies) are also rarely preserved.

As a consequence of their soft bedrock, marl-type terraces seem to be much more ephemeral than the sandstone-type. This is reflected by dating results presented in Normand et al., (2019b) (note that

data are exclusively from Iranian marine terrace sequences). For example, sandstone-type terraces were dated from MIS 5a to MIS 7, implying that terraces at higher altitudes within the same sequence might date back to MIS 17. Marl-type terraces were dated to as young as MIS 3a up to MIS 5a, implying that the highest terraces from those sequence range back to a maximum of MIS 5e. Moreover, the highest marl-type terraces are isolated remnants of less than a square kilometer, compared to their "young" equivalents (MIS 3 to MIS 5a), which are extensive (e.g., Konarak T1 (MIS 5a): 16 km^2, Gurdim T1 (MIS 5a): 13 km^2, Pasabander T2 (MIS3c): 15 km^2) (Normand et al., 2019b) (Fig. 10). Some modern bay beaches are even more extensive, though it is highly uncertain how much of them would be preserved in a future highstand.

Though it is clear that old marl-type terraces are only remnants of their former selves, it is still unsure by which erosive means they were reduced so drastically and so quickly. Wave erosion is a good candidate, since wave attack is directly aimed at the base of the marl cliffs, where any vertical protective effect of a sandstone cap is negligible. However, fallen debris from this cap has been observed to act as protection at the cliff base, hampering wave erosion (e.g., Gurdim terrace (Normand et al., 2019a, Figs. GU)). Surficial subaerial erosion also presumably plays a substantial role in the degradation of marl-type terraces, as attested by observation of finger-like morphologies, which were seemingly formed in response to surface runoff (Fig. 4c, Fig. 8c).

5.4 Coastal evolution patterns

The sandstone-dominated rocky headlands persistently host the coastline through several sea-level highstands as they slowly uplift, developing classical staircase pattern of terraces (Fig. 4a). Marl-type terraces, are more ephemeral but are involved into a positive feedback process during one or two successive highstands. After being uplifted into marine terraces, paleo bay beaches evolve into protruding headlands (e.g., Fig. 7g, Fig. 8e, Fig. 10b), favoring the formation of future sandy bay beaches in the adjacent protected bays (Fig. 10). Ultimately, these sandy beaches will in turn become marine terraces, whereas older terraces will erode and the process will start again.

This behavior can explain the occurrence of lateral or even reverse terrace profiles (Fig. 10). The classical marine terrace sequence pattern is that oldest terraces are situated landwards of younger ones, with terrace limits being roughly parallel to the current coastline; this is the case for Makran sandstone-type terraces. However, Holocene sandy morphologies such as crenulated beaches and tombolos (e.g., Gurdim, Fig. 1) are situated laterally or northwards (i.e., landward) of headlands / marine terraces, setting the stage for the occurrence of reverse terrace profiles. In Jiwani, the lowest (supposedly youngest) marine terrace is situated in the northernmost position relative to the two others (Fig. 10a). We explain this by the formation of crenulated beaches in the lee of the Jiwani headland during successive highstands, as hinted by the curved lineations visible on these Pleistocene terraces as well as the morphologies of Holocene beach ridges in Jiwani bay (Fig. 10a). The supplementary data text B provides some examples of interpreted coastal evolution in different areas of the Makran coast.

6. Conclusion

Our depositional model for the Makran marine terraces based on the terrace morphology, sedimentology and observation of current (Holocene) coastal setting is the following: Wave-cut erosion and platform development occurs during the early stages of a sea-level highstand. This is followed by the deposition of prograding beaches above the eroded platform during the sea-level stillstand and the beginning of the ensuing relative sea-level fall. The deposition of an extensive sedimentary succession above the wave-cut surface is favored by the high sediment input from the

eroding accretionary prism. As such, the Makran marine terraces are best defined as wave-built marine terraces.

The presence of punctuated protruding headlands along the Makran coast is attributed to differential erosion between soft and hard rock. We divide the Makran marine terraces in two groups based on their bedrock lithology. The first are built on locally downfaulted Pliocene sandstone-dominated blocks, outcropping at the coastline, and have a classical staircase morphology. The second are uplifted indurated bay beaches, originally formed on soft marl bedrock between protruding headlands. They are now found as flat-topped topographic anomalies as surrounding uncovered fine-grained bedrock is rapidly eroded down to the coastal plain level. As old beaches are uplifted into headlands, they influence the formation of the future generations of beaches during the ensuing highstand.

Our study shows that the morphology of the Makran coast was strongly modulated by competing interactions between three main factors. 1) Tectonic forces, providing regional relative sea-level fall (together with eustatism), while juxtaposing units of markedly different erodability to the same structural level by faulting. 2) Surface processes such as differential erodibility, responsible for the isolation of protruding headlands and the high sedimentary input at the Makran coast. 3) Coastal processes, permitting the wave-erosion of marine terraces and the development of extensive beaches.

Data availability

Supplementary data for this paper are found in the following repository: https://doi.org/10.5281/zenodo.2558349 (Normand et al., 2019a). These are additional field pictures illustrating the paper, together with their legends and geolocalisations.

Acknowledgements

This work was funded by the Swiss National Science Foundation, project n°200021_155904. We thank Kevin Pedoja for his input and all the fruitful and interesting discussions. We are also grateful to Reza Ensani, Feisal Arjomandi, Nurrudin Mazarzehi, Yousef Adeeb and Gholamreza Hosseinyar for helping us with logistics in Iran and accompanying us in the field.

Author contribution

RN did the fieldwork, wrote the paper and created the figures. GS accompanied him in the field and had substantial input on the tectonic and geodynamic aspects. AB provided his input on Iranian geology and tectonics and organized field campaigns.

The authors declare that the research was conducted in the absence of any commercial **or financial** relationships that could be construed as a potential conflict of interest.

References

Anderson, R.S., Densmore, A.L., and Ellis, M.A., 1999, The generation and degradation of marine terraces. Basin Research, v. 11, no. 1, p. 7–19, doi: 10.1046/j.1365-2117.1999.00085.x.

Bird, E., 2000, Coastal Geomorphology, an introduction: Wiley.

Bourget, J., Zaragosi, S., Ellouz-Zimmermann, S., Ducassou, E., Prins, M.A., Garlan, T., Lanfumey, V., Schneider, J.L., Rouillard, P., and Giraudeau, J., 2010, Highstand vs. lowstand turbidite system growth in the Makran active margin: Imprints of high-frequency external controls on sediment

delivery mechanisms to deep water systems. Marine Geology, v. 274, no. 1–4, p. 187–208, doi: 10.1016/j.margeo.2010.04.005.
Byrne, D.E., Sykes, L.R., and Davis, D.M., 1992, Great Thrust Earthquakes and Aseismic Slip Along the Plate Boundary of the Makran Subduction Zone. Journal of Geophysical Research-Solid Earth, v. 97, p. 449–478, doi: 10.1029/91JB02165.
Catuneanu, O., Galloway, W.E., Kendall, C.G.S.C., Miall, A.D., Posamentier, H.W., Strasser, A., and Tucker, M.E., 2011, Sequence Stratigraphy : Methodology and Nomenclature. Newsletters on Stratigraphy, v. 44/3, no. November, p. 173–245, doi: 10.1127/0078-0421/2011/0011.
Dietz, R., 1963, Wave-Base, Marine Profile of Equilibrium, and Wave-Built Terraces: A Critical Appraisal. Geological Society of America Bulletin, v. 74, p. 971–990.
Dolati, A., and Burg, J.-P., 2012, Preliminary fault analysis and paleostress evolution in the Makran Fold-and-Thrust Belt in Iran, *in* Al Hosani, K., Roure, F., Ellison, R., and Lokier, S. eds., Lithosphere Dynamics and Sedimentary Basins: The Arabian Plate and Analogues, Springer, p. 261–277.
Dupré, W.R., 1984, Reconstruction of paleo-wave conditions during the Late Pleistocene from marine terrace deposits, Monterey Bay, California. Marine Geology, v. 60, p. 435–454.
Ellouz-Zimmermann, N., Lallemant, S.J., Castilla, R., Mouchot, N., Leturmy, P., Battani, A., Buret, C., Cherel, L., Desaubliaux, G., Deville, E., Ferrand, J., Lügcke, A., Mahieux, G., Mascle, G., et al., 2007, Offshore Frontal part of the Makran Accretionary Prism: The Chamak Survey (Pakistan), *in* Lacombe, O., Roure, F., Lavé, J., and Vergés, J. eds., Thrust belts and Foreland Basins, Springer, Berlin, p. 351–366.
England, P., and Molnar, P., 1990, Surface uplift, uplift of rocks, and exhumation of rocks. Geology, v. 18, no. 12, p. 1173–1177, doi: 10.1130/0091-7613(1990)018<1173:SUUORA>2.3.CO.
Falcon, N.L., 1947, Raised beaches and terraces of the Iranian Makran coast. The Geographical Journal, v. 109, no. 1, p. 149–151.
Farhoudi, G., and Karig, D.E., 1977, Makran of Iran and Pakistan as an active arc system. Geology, v. 5, no. 11, p. 664–668, doi: 10.1130/0091-7613(1977)5<664:MOIAPA>2.0.CO;2.
Frohling, E., and Szeliga, W., 2016, GPS constraints on interplate locking within the Makran subduction zone. Geophysical Journal International, v. 205, p. 67–76, doi: 10.1093/gji/ggw001.
Gharibreza, M., 2016, Evolutionary trend of paleoshorelines in the Coastal Makran zone (Southeast Iran) since the mid-Holocene. Quaternary International, v. 392, p. 203–212, doi: 10.1016/j.quaint.2015.06.030.
Ghorashi, M., 1978, Late Cainozoic faulting in S.E. Iran: PhD Thesis, University College London, 289 p.
Gilbert, G.., 1890, Lake Bonneville: US. Geological Survey Monograph.
Grando, G., and McClay, K., 2007, Morphotectonics domains and structural styles in the Makran accretionary prism, offshore Iran. Sedimentary Geology, v. 196, p. 157–179, doi: 10.1016/j.sedgeo.2006.05.030.
Haghipour, N., Burg, J.P., Ivy-Ochs, S., Hajdas, I., Kubik, P., and Christl, M., 2014, Correlation of fluvial terraces and temporal steady-state incision on the onshore Makran accretionary wedge in southeastern Iran: Insight from channel profiles and 10Be exposure dating of strath terraces. Bulletin of the Geological Society of America, v. 127, no. 3–4, p. 560–583, doi: 10.1130/B31048.1.
Harms, J.C., Cappel, H.N., and Francis, D.C., 1984, The Makran Coast of Pakistan: It's Stratigraphy and Hydrocarbon Potential, *in* Haq, B.U. and Milliman, J.D. eds., Marine Geology and Oceanography of Arabian Sea and Coastal Pakistanography of Arabian Sea and Coastal Pakistan, Van Nostrand Reinhold Company Inc., p. 3–26.
Hurst, M.D., Barkwith, A., Ellis, M.A., Thomas, C.W., and Murray, A.B., 2015, Exploring the sensitivities of crenulate bay shorelines to wave climates using a new vector-based one-line model. Journal of Geophysical Research: Earth Surface, p. 2586–2608, doi: 10.1002/2015JF003704.We.

Hurst, M.D., Rood, D.H., Ellis, M.A., Anderson, R.S., and Dornbusch, U., 2016, Recent acceleration in coastal cliff retreat rates on the south coast of Great Britain. Proceedings of the National Academy of Sciences, v. 113, no. 47, p. 13336–13341, doi: 10.1073/pnas.1613044113.

Jara-Muñoz, J., and Melnick, D., 2015, Unraveling sea-level variations and tectonic uplift in wave-built marine terraces, Santa María Island, Chile. Quaternary Research (United States), v. 83, no. 1, p. 216–228, doi: 10.1016/j.yqres.2014.10.002.

Khan, M.A., Bendick, R., Bhat, M.I., Bilham, R., Kakar, D.M., Khan, S.F., Lodi, S.H., Qazi, M.S., Singh, B., Szeliga, W., and Wahab, A., 2008, Preliminary geodetic constraints on plate boundary deformation on the western edge of the Indian plate from TriGGnet (Tri-University GPS Geodesy Network). Journal of Himalayan Earth Sciences, v. 41, p. 71–87.

Lajoie, K.R., 1986, Coastal Tectonics, *in* Wallace, R. ed., Active Tectonics: Impact on Society, Washington DC: National Academy Press, p. 95–124.

Leggett, J.K., and Platt, J.P., 1984, Structural Features of the Makran Fore-arc on Landsat Imagery, *in* Haq, B.U. and Milliman, J.D. eds., Marine Geology and Oceanography of Arabian Sea and Coastal Pakistan, Van Nostrand Reinhold Company Scientific and Academic Editions, p. 33–43.

Limber, P.W., Murray, A.B., Adams, P.N., and Goldstein, E.B., 2014, Unraveling the dynamics that scale cross-shore headland relief on rocky coastlines: 1. Model development. Journal of Geophysical Research: Earth Surface, v. 119, p. 854–873, doi: 10.1002/2013JF002950.

Little, R.D., 1972, Terraces of the Makran Coast of Iran and parts of West Pakistan: PhD Thesis, University of Southern California, 168 p.

Masson, F., Anvari, M., Djamour, Y., Walpersdorf, A., Tavakoli, F., Daignières, M., Nankali, H., and Van Gorp, S., 2007, Large-scale velocity field and strain tensor in Iran inferred from GPS measurements: New insight for the present-day deformation pattern within NE Iran. Geophysical Journal International, v. 170, no. 1, p. 436–440, doi: 10.1111/j.1365-246X.2007.03477.x.

McCall, G.J.H., and Kidd, R.G., 1982, The Makran, Southeastern Iran: the anatomy of a convergent plate margin active from Cretaceous to Present (J. K. Leggett, Ed.). Geological Society, London, Special Publications, v. 10, p. 387–397.

Normand, R., Simpson, G., and Bahroudi, A., 2019a, Data for: Pleistocene coastal evolution of the Makran subduction zone. , doi: 10.5281/zenodo.2558349.

Normand, R., Simpson, G., Herman, F., Biswas, R.H., Bahroudi, A., and Schneider, B., 2019b, Dating and morpho-stratigraphy of uplifted marine terraces in the Makran subduction zone (Iran). Earth Surface Dynamics, v. 7, p. 321–344, doi: 10.5194/esurf-7-321-2019.

Page, W.D., Alt, J.N., Cluff, L.S., and Plafker, G., 1979, Evidence for the recurrence of large-magnitude earthquake along the Makran coast of Iran and Pakistan. Tectonophysics, v. 52, p. 533–547, doi: 10.1016/0040-1951(79)90269-5.

Platt, J.P., and Leggett, J.K., 1986, Stratal Extension in Thrust Footwalls, Makran Accretionary Prism: Implications for Thrust Tectonics. American Association of Petroleum Geologists Bulletin, v. 70, no. 2, p. 191–203.

Rajendran, C.P., Rajendran, K., Shah-hosseini, M., Beni, A.N., Nautiyal, C.M., and Andrews, R., 2013, The hazard potential of the western segment of the Makran subduction zone, northern Arabian Sea. Natural Hazards, v. 65, no. 1, p. 219–239, doi: 10.1007/s11069-012-0355-6.

Regard, V., Dewez, T., Bourlès, D.L., Anderson, R.S., Duperret, A., Costa, S., Leanni, L., Lasseur, E., Pedoja, K., and Maillet, G.M., 2012, Late Holocene seacliff retreat recorded by 10Be profiles across a coastal platform: Theory and example from the English Channel. Quaternary Geochronology, v. 11, p. 87–97, doi: 10.1016/j.quageo.2012.02.027.

Reyss, J.L., Pirazzoli, P.A., Haghipour, A., Hatté, C., and Fontugne, M., 1998, Quaternary marine terraces and tectonic uplift rates on the south coast of Iran. Geological Society, London, Special Publications, v. 146, p. 225–237, doi: 10.1144/GSL.SP.1999.146.01.13.

Saket, A., and Etemad-shahidi, A., 2012, Wave energy potential along the northern coasts of the Gulf of Oman , Iran. Renewable Energy, v. 40, no. 1, p. 90–97, doi: 10.1016/j.renene.2011.09.024.
Samadian, M.R., Ghomashi, A., Chaichi, Z., Eshraghi, S.A., Kholghi, M.H., Abdollahi, M.R., Sohaili, M., and Korei, M.T., 2004, Geological map of Iran 1:100'000 : Peersohrab sheet: Geological Survey of Iran.
Samadian, M.R., Ghomashi, A., Jamshidi, K., Afsharianzadeh, A., Sharifian, M.I., Abdolahi, M.R., Eghlimi, B., and Ahmadzadeh Heravi, M., 1994, Geological map of Iran 1:100'000 : Kahir sheet: Geological Survey of Iran.
Samadian, M.R., Ghomashi, A., Mohebbi, A.R., Jafarian, M.B., Abdoli, M., and Ahmadzadeh Heravi, M., 1996, Geological map of Iran 1:100'000 : Chabahar sheet: Geological Survey of Iran.
Sanlaville, P., Besenval, R., Evin, J., and Prieur, A., 1991, Evolution de la région littorale du Makran pakistanais à l'Holocène. Paléorient, v. 17, no. 1, p. 3–18, doi: 10.3406/paleo.1991.4536.
Shah-Hosseini, M., Ghanavati, E., Morhange, C., Naderi Beni, A., Lahijani, H.A., and Hamzeh, M.A., 2018, The evolution of Chabahar beach ridge system in SE Iran in response to Holocene relative sea level changes. Geomorphology, v. 318, p. 139–147, doi: 10.1016/j.geomorph.2018.06.009.
Snead, R.J., 1967, Recent Morphological changes along the coast of West Pakistan. Annals of the Association of American Geographers, v. 57, no. 3, p. 550–565, doi: 10.1111/j.1467-8306.1967.tb00621.x.
Snead, R.J., 1993, Uplifted Marine Terraces along the Makran coast of Pakistan and Iran, *in* Shroder, J.F.J. ed., Himalaya to the Sea, Routledge, London, p. 327–362.
Tamura, T., 2012, Beach ridges and prograded beach deposits as palaeoenvironment records. Earth-Science Reviews, v. 114, p. 279–297, doi: 10.1016/j.earscirev.2012.06.004.
Trenhaile, A.S., 2002, Modeling the development of marine terraces on tectonically mobile rock coasts. Marine Geology, v. 185, no. 3–4, p. 341–361, doi: 10.1016/S0025-3227(02)00187-1.
Trenhaile, A.S., 2000, Modeling the development of wave-cut shore platforms. Marine Geology, v. 166, no. 1–4, p. 163–178, doi: 10.1016/S0025-3227(00)00013-X.
Valvo, L.M., Murray, A.B., and Ashton, A., 2006, How does underlying geology affect coastline change ? An initial modeling investigation. Journal of Geophysical Research, v. 111, no. F02025, doi: 10.1029/2005JF000340.
Vernant, P., Nilforoushan, F., Hatzfeld, D., Abbassi, M.R., Vigny, C., Masson, F., Nankali, H., Martinod, J., Ashtiani, A., Bayer, R., Tavakoli, F., and Chéry, J., 2004, Present-day crustal deformation and plate kinematics in the Middle East constrained by GPS measurements in Iran and northern Oman. Geophysical Journal International, v. 157, no. 1, p. 381–398, doi: 10.1111/j.1365-246X.2004.02222.x.
Vita-Finzi, C., 1980, 14C Dating of recent crustal movements in the Persian Gulf and Iranian Makran. Radiocarbon, v. 22, no. 3, p. 763–773, doi: 10.1017/S0033822200010134.
Vita-Finzi, C., 1981, Late Quaternary deformation on the Makran coast of Iran. Zeitschrift für Geomorphologie, Supplementary Issues, v. 40, p. 213–226.
Vita-Finzi, C., 1975, Quaternary Deposits in the Iranian Makran. The Geographical Journal, v. 141, no. 3, p. 415–420, doi: 10.2307/1796475.
White, R.S., and Louden, K.E., 1982, The Makran continental margin: structure of a thickly sedimented convergent plate boundary, *in* Watkins, J.S., Drake, C.L. ed., AAPG Special Volumes, Studies in Continental Margin Geology, p. 499–518.
Yasso, W.E., 1965, Plan Geometry of Headland-Bay Beaches. The Journal of Geology, v. 73, no. 5, p. 702–714, doi: 10.1086/627111.

Figure and table captions

Figure 1. General location of the Makran Subduction zone. A: Satellite image of a portion of the coastal Makran near Chabahar region (SE Iran). Image: Landsat. Black lines are beach ridges. Black names are localities. Headlands host marine terraces. B: Shaded relief (SRTM) of Fig. 1a (dark blue = 0m, red = 700m altitude). Notice the flat coastal plain and the protruding headlands at the coastline.

Figure 2. Simplified bedrock lithology map of the Chabahar region, emphasizing location of Marl or sandstone dominated lithologies. Except from Chabahar headland, Pliocene outcrops are inferred.

Figure 3. Major normal faults bordering Chabahar headland. A-D: Photo and sketch of the outcropping faults. The low-lying coastal plain sits in the uplifted block, whereas the headland is downthrown. E-F: A major normal fault outcropping within the headland. G: Localization of the major normal faults of Chabahar headland (red). Grey fault is inferred. H: Sketch of a profile from the Makran ranges to the sea, going through a downfaulted headland (as in profile X-Y in Fig. 3g). Tectonic deformation of the Tertiary layers is ignored for simplicity.

Figure 4. Figures illustrating the Mmt geomorphology and sedimentology. More pictures may be found in (Normand et al., 2019a). A: General view of sandstone-dominated terraces, which have a classic staircase morphology. Here, two terraces of Lipar T1 and T3 are separated by a paleocliff. The Holocene platform is being carved through both T1 and T3, and megaboulders are seen embedded in the small Holocene beach at the feet of T3. T3 is 60m high. Red square is the position of Fig. 4b. (25.250°N, 60.839°E; looking SE). B: Close up of the vicinity of the Lipar T1 shoreline angle. Notice the angular unconformity with the bedrock bedding (blue lines) and the fossil version of embedded megaboulders at the foot of the paleocliff (which is situated a few meters to the left of the picture). (25.247°N, 60.848°E). C: Google Earth satellite image of Tang T3, illustrating some morphological properties of marl-type terraces, such as the isolated platform morphology, the finger-like protrusion and the curved aspect, emphasized by lineations on the terrace surface (see also Fig. 8g). (25.42°N, 59.88°E). D: Northern side of Pasabander T3. Note the absence of paleocliff and the highly degraded marl bedrock where unprotected by the terrace deposits. (25.134°N, 61.449°E). E: Example of terrace deposit succession (here, section P8 of Fig. 6a). (25.077909°N, 61.354360°E).

Figure 5. Legend of the logs in Fig. 6.

Figure 6. Sedimentary logs of the terrace deposits and their location. A: Sedimentary logs, arranged from shoreline angle (top of the picture) to seawards side (bottom). Colors of the background correspond to the terrace region from which they were measured (see maps). Legends are found in Fig. 5. * For facies description, see Table 1. ** SA: shoreline angle, ESA: eroded shoreline angle (when the paleocliff is eroded, see Fig. 4d and Fig. 7f), MT: middle of the terrace, SS: sea side of the terrace. B to E: Localization of the logs of Gurdim (turquoise), Konarak (blue), Chabahar (green), Ramin (red), Lipar (yellow) and Pasabander (purple).

Figure 7. Interpretation of Makran marine terrace development as sea-level varies through time. A-D: Model for sandstone-type terraces. A: Start of the highstand, carving of the wave-cut platform. B: Post peak of the highstand, start of beach deposition, as seen currently in the Makran (e.g.: Fig. 4a foreground). C: End of highstand, start of sea-level fall. Rapid beach progradation across the whole platform. D: Next highstand, after relative sea-level fall, the paleobeach is now found as a marine terrace. The paleocliff seems to be eroding further after platform abandonment, as its current position can be a few tens of meters from the megaboulders (Normand et al., 2019a, images CH5-6 and LI4). E-F: Model for marl-type marine terraces. E: After platform carving into the soft marl, the bay beach develops in a series of prograding beach ridges, as seen currently along the Makran (e.g.: Fig. 1, Fig.

7g). Notice the difference in lateral extension compared to sandstone-type terraces. F: Situation at the next highstand, the beach is uplifted into a marine terrace (e.g.: Fig. 4b). G: Satellite image (Bing) of Pozm bay and surroundings, illustrating modern equivalents of some of these sketches. More examples illustrating these profiles in Fig. 8 and 9.

Figure 8. Marl-type beaches and terraces. Bedrock and terrace maps legends are similar to Fig. 2, plus: light grey: coastal plain, yellow polygons: Holocene beaches, black lines: Holocene beach ridges, blue dashed lines: paleo beach ridges. Colored profiles are the sketches from Fig. 7. A-B: Pishukan beach (Pakistan), a Holocene bay beach built on marl bedrock. Notice the sharp northern beach limit carved by wave erosion. C-D: Ras Shamal Bandar, a terrace ~50km west of the village of Pasni (Pakistan). Notice the morphological similarities with Pishukan beach pictured in Fig. 8a, though here, the paleocliff and badlands beyond are eroded down to the coastal plain level. E-F: Tang terraces. T3 is an uplifted version of the Holocene beach (yellow in Fig. 8f), notice the morphological similarities. While the Holocene beach is deposited in the leer of T1, T3 was created in a similar fashion, by wave-diffraction around a rocky headland (probably the one outcropping in the east of the picture). G-H: Pasabander marl-type terraces; T2, T3 and T4. The morphology of T2 is similar to the crenulated Holocene bay beaches (e.g.: Fig. 7g, 8e), and was probably built by wave-diffraction. Fig. 8f and 8h inspired from the maps of (Normand et al., 2019b).

Figure 9. Differential erosion of the marl-bedrock marine terraces and the implications for surface uplift rates. Slvl = sea level. Vertical scale exaggerated.

Figure 10. Two examples of Makran coastal evolution models over several sea-level highstands. The presence of headlands in the form of sandstone-dominated bedrock outcrops (Jiwani) or uplifted marine terraces (Pasabander) has favored the creation of crenulated bay beaches, later uplifted into marine terraces, which in turn act as headlands. A: Jiwani terraces coastal evolution (highstand ages are inferred, since no dating results are available). Current situation is presented with a satellite image (Landsat) and interpreted terrace map. The topographic profile (A-B) through the terraces is not the expected classical staircase-like profile. B: Pasabander terraces coastal evolution. * Ages from OSL dating of Normand et al. (2019b). Current situation is presented with a satellite image (Landsat), interpreted terrace map (modified after Normand et al. (2019b)) and topographic profile C-D.

Table.1 Facies encountered in the western Makran marine terrace sedimentary successions

Facies	Matrix Grain-size	Bioclasts	Other clasts	Support	Sedimentary structures
A	Sand	Roots		Matrix-supp.	High angle, large cross strat.
B	Sand	Shells or shell fragments	A few small pebbles	Matrix-supp.	Horizontal lamination. Some small scale trough cross strat.
C	Sand	Shells or shell fragments	A few pebbles	Matrix-supp.	Trough cross strat., foresets
D	Silt to clay	Shells or shell fragments	Pebbles, bored pebbles	Matrix-supp.	None
E	Sand to clay	Shell fragments	10-50 cm boulders, pebbles	Clast-supp.	None
F	Sand	Shell fragments	Pebbles (1-8 cm diamater)	Both	None, or pebbles imbrication

Facies	Biorturbation	Sorting	Others	Interpretation
A	Tubular burrows	Very good	Rarerly observed (1 occurrence)	Eolian
B	Tubular burrows	Good	Laminations gently sloping towards the sea	Beach / swash deposits
C	None	Good	High energy deposits	Wave-influenced, energetic environment / Shoreface
D	Important	Bad		Lagoonal deposits
E	None	Very bad	Bored pebbles	Transgressive surface (ravinement)
F	None	Bad	Pebble rich deposit, both occurrences of clast and matrix supported	River influenced deposit (mouth bar?)

642

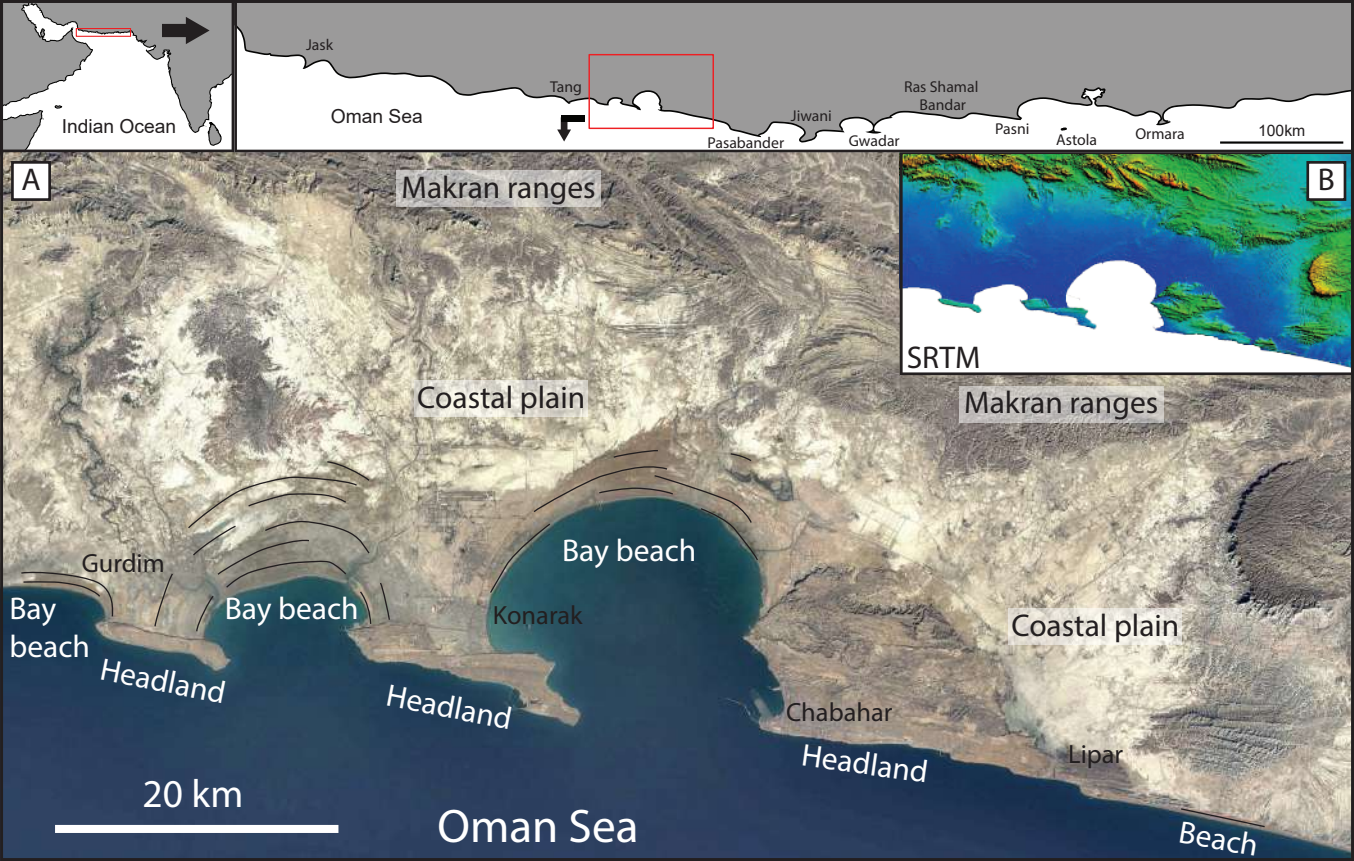
Indian Ocean
Jask
Oman Sea
Tang
Jiwani
Pasabander
Gwadar
Ras Shamal
Bandar
Pasni
Astola
Ormara
100km
A
Makran ranges
B
SRTM
Coastal plain
Makran ranges
Gurdim
Bay beach
Bay beach
Bay beach
Konarak
Coastal plain
Headland
Headland
Chabahar
Headland
Lipar
20 km
Oman Sea
Beach

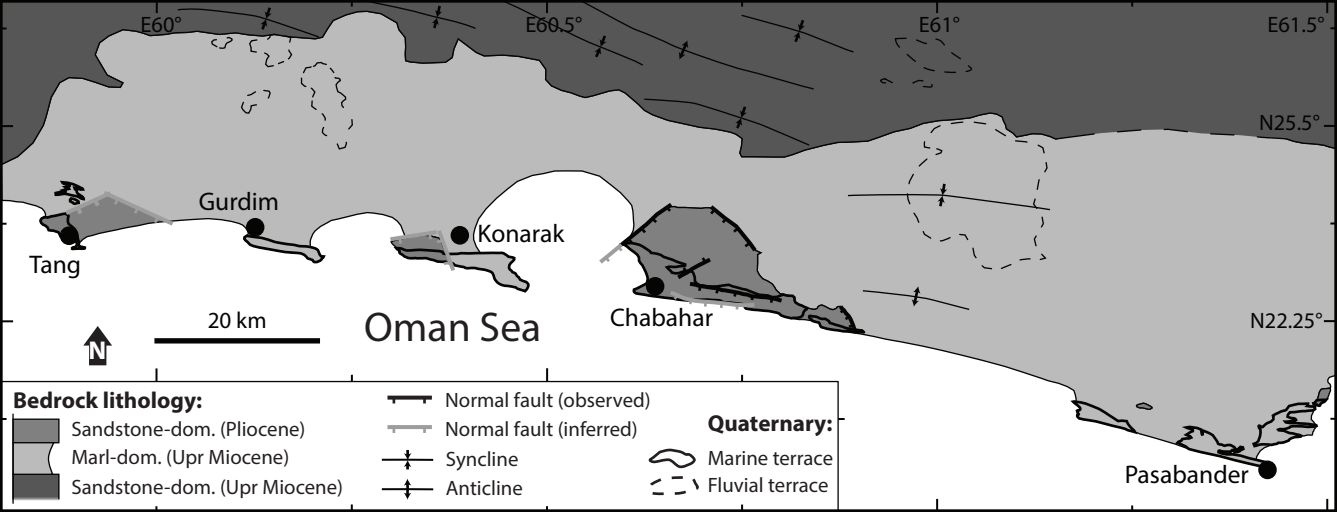
E60°
E60.5°
E61°
E61.5°
N25.5°
N22.25°
Gurdim
Konarak
Tang
Chabahar
Pasabander
20 km
Oman Sea
N
Bedrock lithology:
Sandstone-dom. (Pliocene)
Marl-dom. (Upr Miocene)
Sandstone-dom. (Upr Miocene)
Normal fault (observed)
Normal fault (inferred)
Syncline
Anticline
Quaternary:
Marine terrace
Fluvial terrace


NE
SW
A


SE
NW
C


NW
SE
E

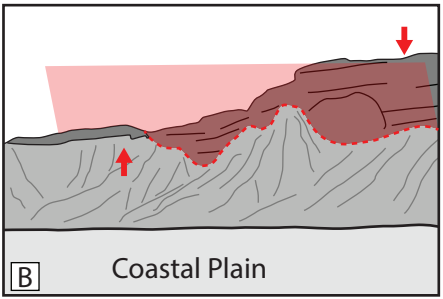
B
Coastal Plain

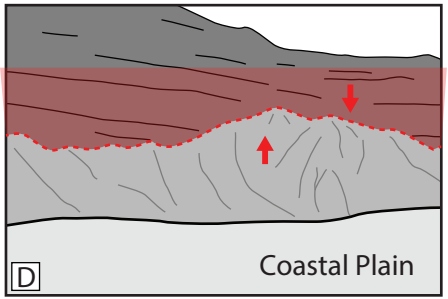
D
Coastal Plain

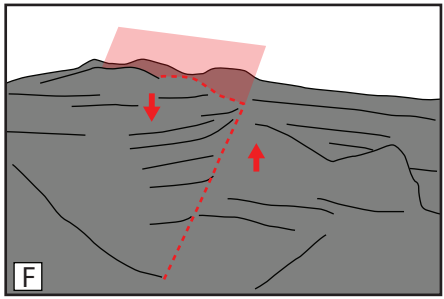
F

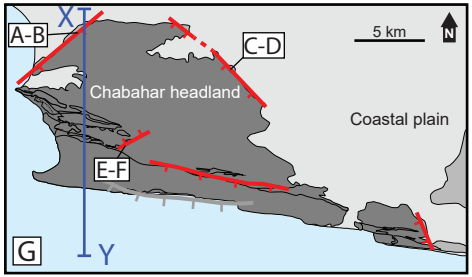
A-B
X
T
C-D
5 km
N
Chabahar headland
Coastal plain
E-F
G
Y

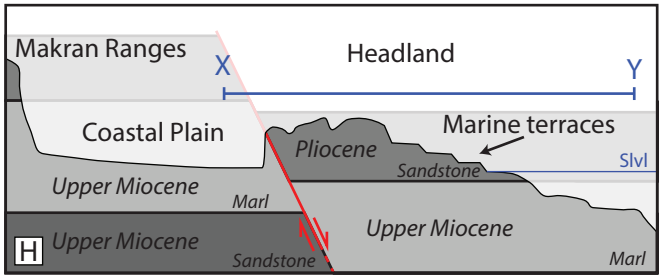
Makran Ranges
X
Headland
Y
Coastal Plain
Marine terraces
Pliocene
Sandstone
SlvI
Upper Miocene
Marl
H
Upper Miocene
Upper Miocene
Sandstone
Marl

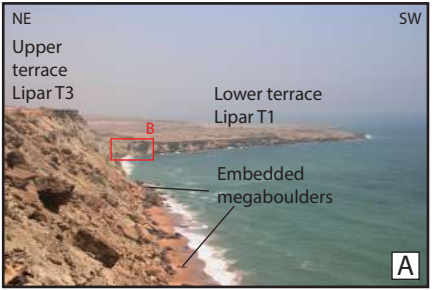
NE
SW
Upper terrace Lipar T3
Lower terrace Lipar T1
B
Embedded megaboulders
A

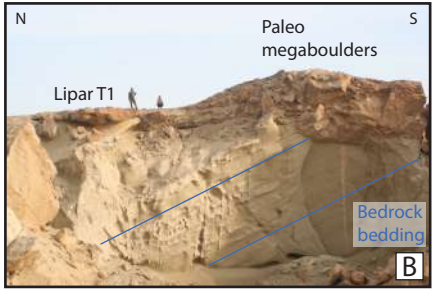
N
S
Paleo megaboulders
Lipar T1
Bedrock bedding
B

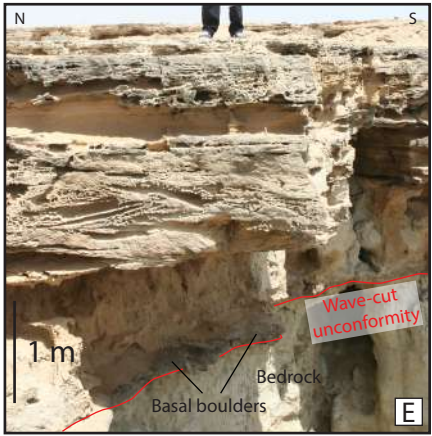
N
S
Wave-cut unconformity
1 m
Bedrock
Basal boulders
E

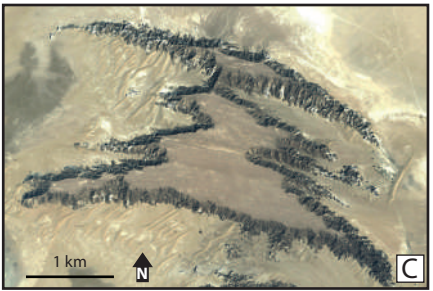
1 km
N
C


SW
NE
Pasabander T3
Coastal plain
D

Logs legend

Lithology

Marl

Bedrock Terrace

Sandstone

Bedrock Terrace

Through cross stratifications

Parallel, low angle stratification

High angle cross stratifications

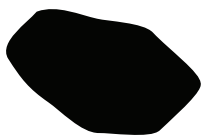

Meter(s) sized megaboulder(s)

Erosive surface

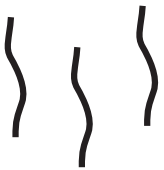

Bioturbation

Roots

Shells / Shell fragments

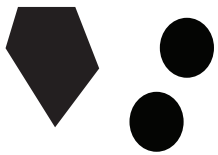

Angular / rounded boulders or pebbles

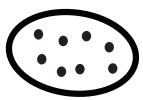

Bored pebbles

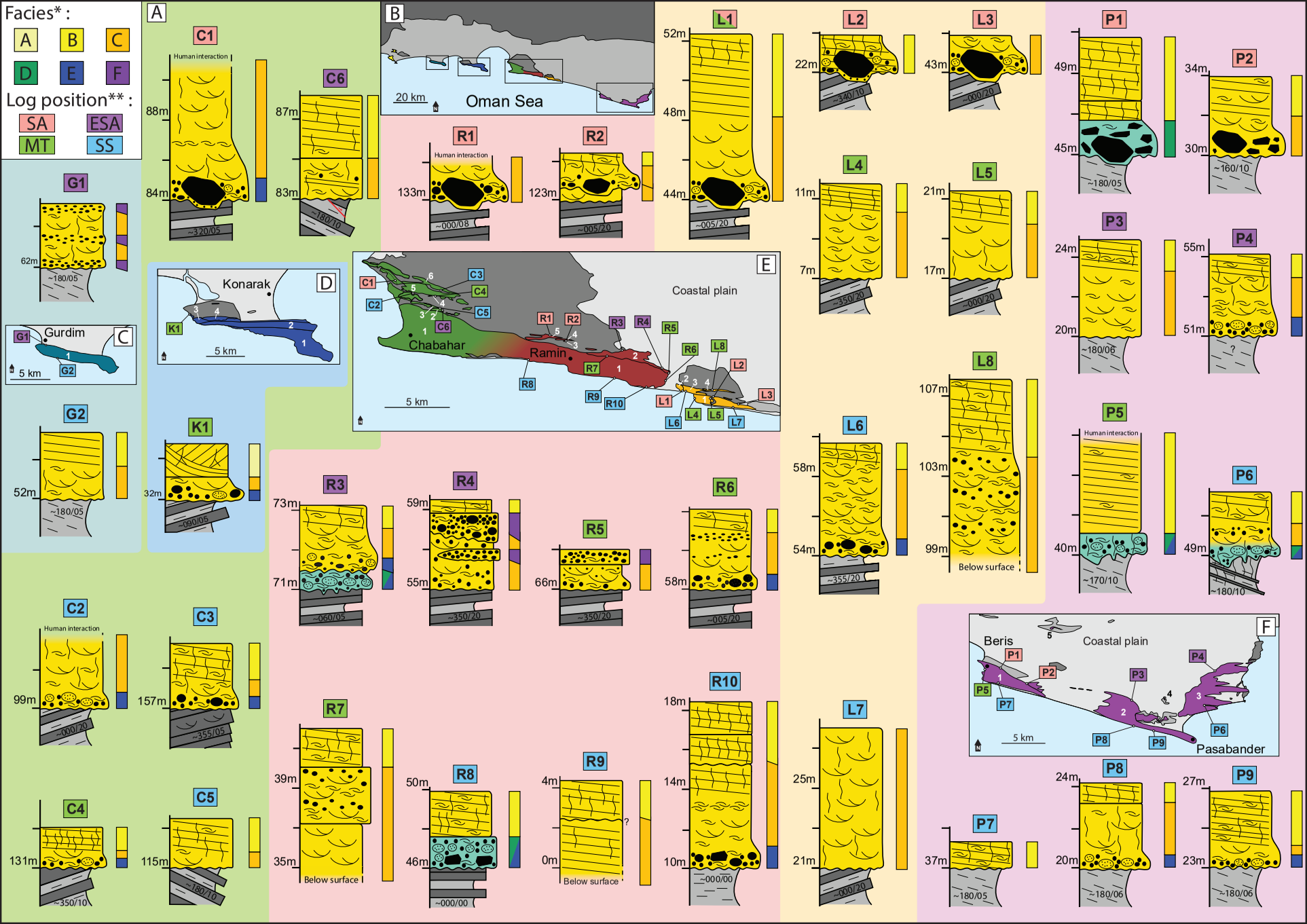
Facies* :
A
B
C
D
E
F
Log position** :
SA
ESA
MT
SS
A
B
C
D
E
F
Oman Sea
20 km
Konarak
5 km
Gurdim
5 km
Coastal plain
Chabahar
Ramin
5 km
Beris
Coastal plain
Pasabander
5 km
Human interaction
Below surface
C1
C2
C3
C4
C5
C6
G1
G2
K1
R1
R2
R3
R4
R5
R6
R7
R8
R9
R10
L1
L2
L3
L4
L5
L6
L7
L8
P1
P2
P3
P4
P5
P6
P7
P8
P9

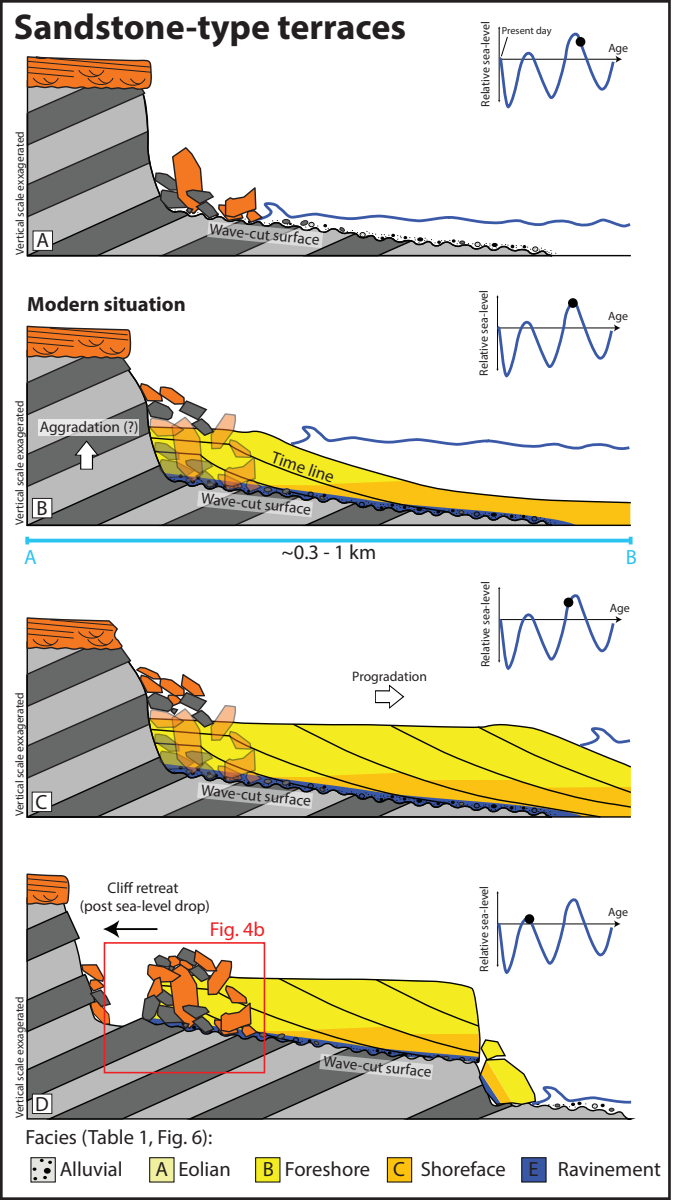
Sandstone-type terraces
Present day
Relative sea-level
Age
Vertical scale exaggerated
A
Wave-cut surface
Modern situation
Aggradation (?)
Time line
Wave-cut surface
B
A
~0.3 - 1 km
B
Progradation
C
Cliff retreat
(post sea-level drop)
Fig. 4b
D
Facies (Table 1, Fig. 6):
Alluvial
A Eolian
B Foreshore
C Shoreface
E Ravinement

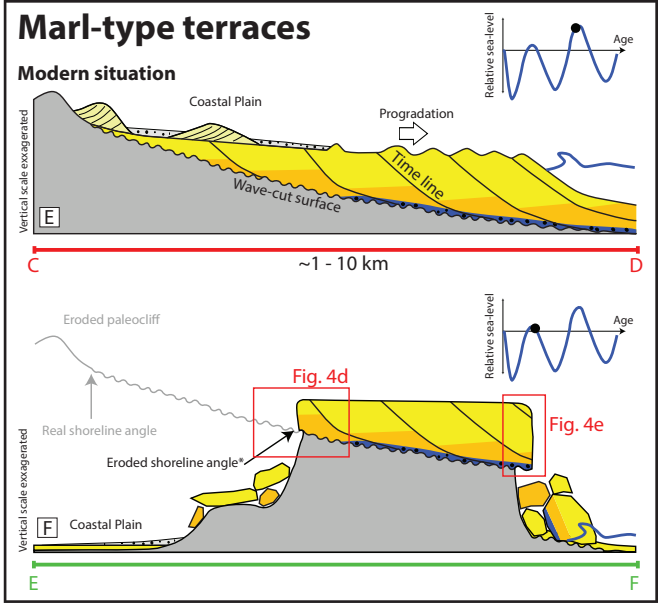
Marl-type terraces
Modern situation
Coastal Plain
Progradation
Time line
Wave-cut surface
E
C
~1 - 10 km
D
Eroded paleocliff
Fig. 4d
Fig. 4e
Real shoreline angle
Eroded shoreline angle*
F
Coastal Plain
E
F

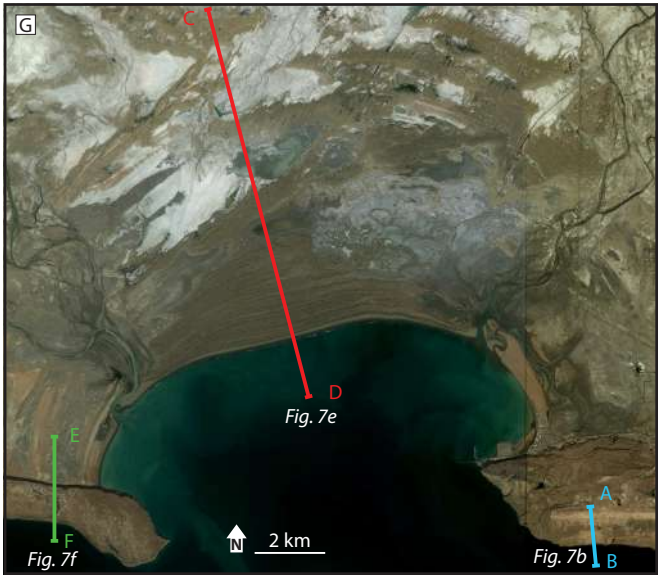
G
C
D
Fig. 7e
E
F
Fig. 7f
N
2 km
A
B
Fig. 7b

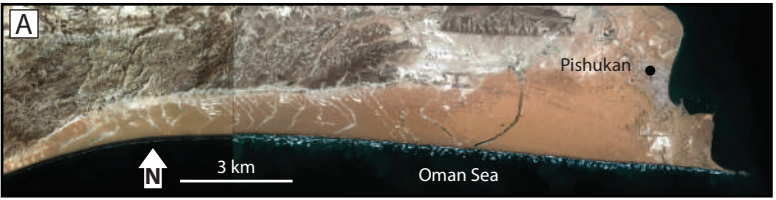
A
Pishukan
N
3 km
Oman Sea

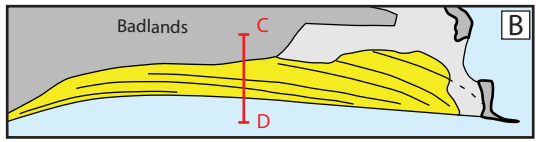
Badlands
C
B
D

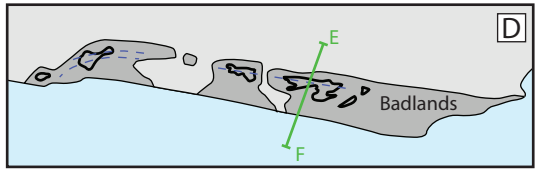
D
E
Badlands
F


C
Coastal Plain
Pasni, 50 km
N
5 km
Oman Sea

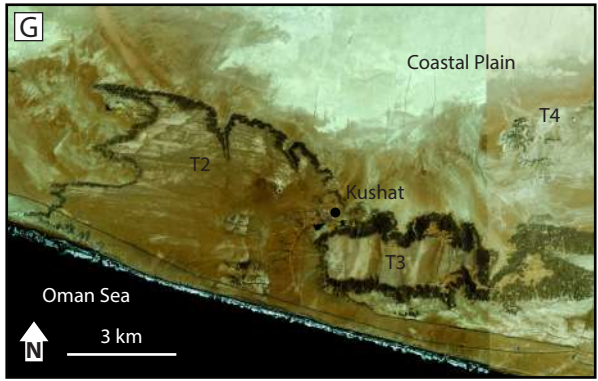
G
Coastal Plain
T4
T2
Kushat
T3
Oman Sea
N
3 km


E
Coastal Plain
T3
T2
T1
Tang
Oman Sea
N
3 km

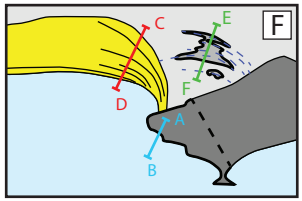
C
E
F
D
A
B

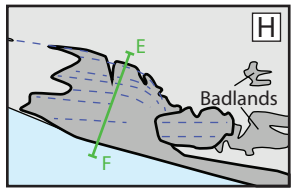
H
E
Badlands
F

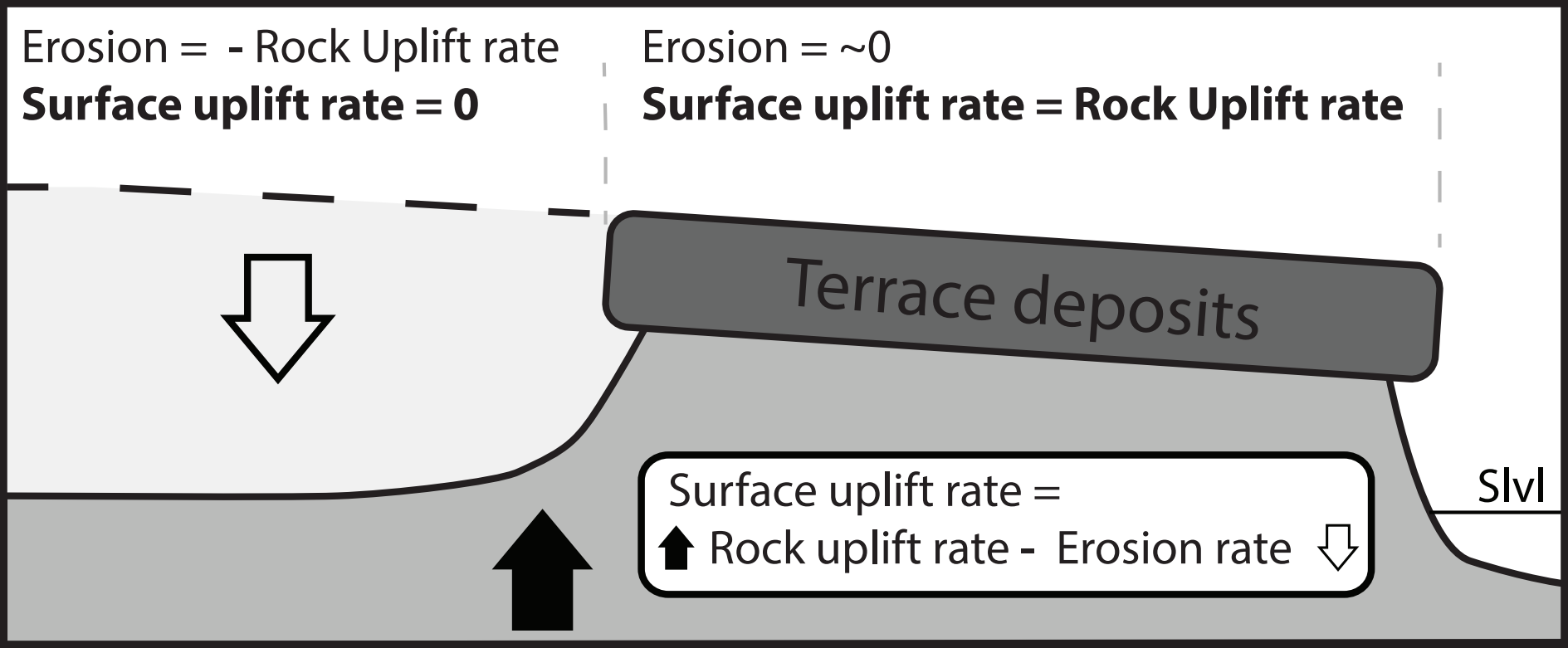
Erosion = - Rock Uplift rate
Surface uplift rate = 0
Erosion = ~0
Surface uplift rate = Rock Uplift rate
Terrace deposits
Surface uplift rate =
Rock uplift rate - Erosion rate
SlvI

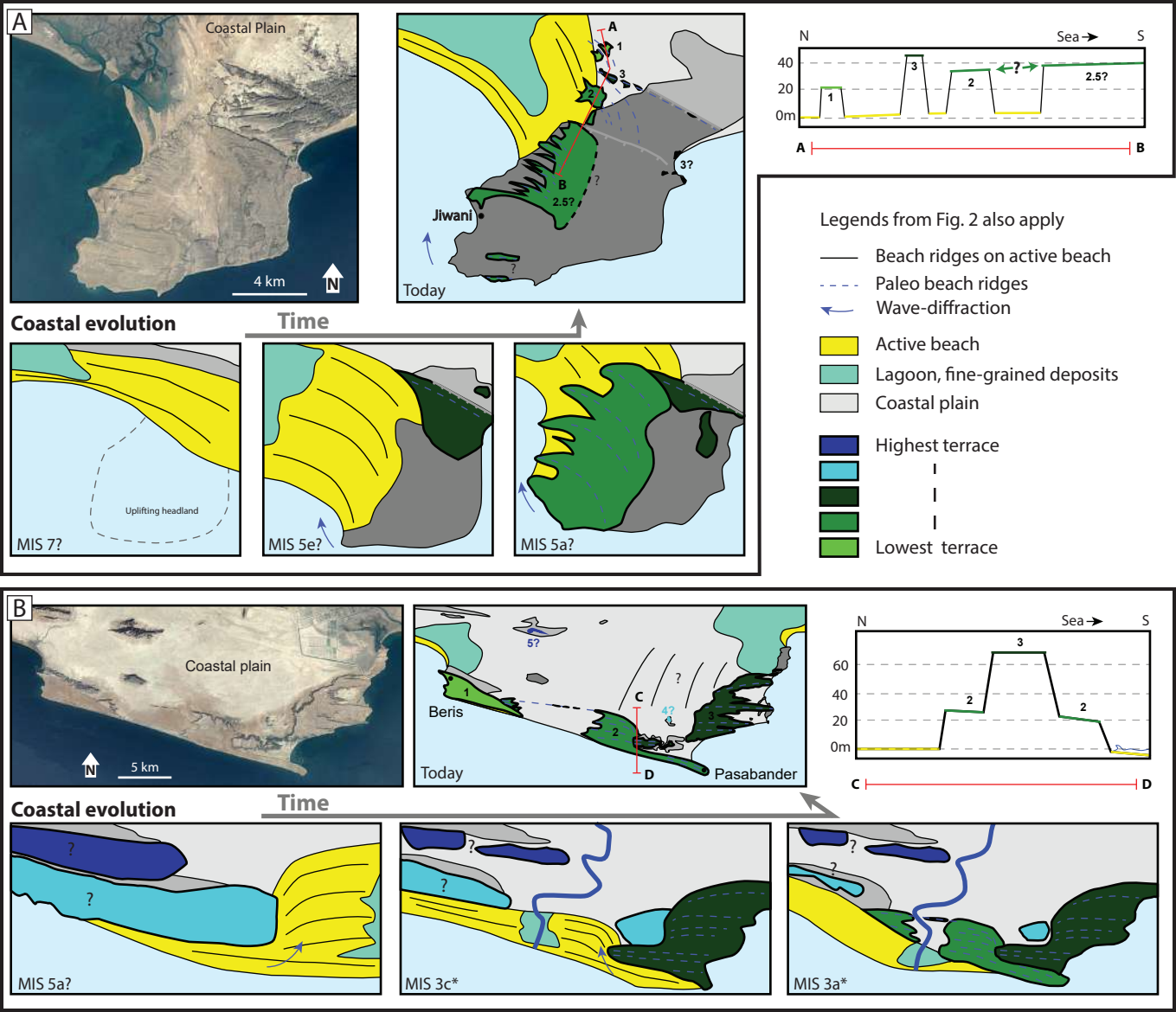
A
Coastal Plain
4 km
N
A
1
3
2
B
2.5?
3?
Jiwani
Today
N
Sea
S
40
20
0m
1
3
2
?
2.5?
A
B
Coastal evolution
Time
Uplifting headland
MIS 7?
MIS 5e?
MIS 5a?
Legends from Fig. 2 also apply
Beach ridges on active beach
Paleo beach ridges
Wave-diffraction
Active beach
Lagoon, fine-grained deposits
Coastal plain
Highest terrace
I
I
I
Lowest terrace
B
Coastal plain
N
5 km
5?
1
Beris
C
4?
2
D
Today
Pasabander
N
Sea
S
60
40
20
0m
3
2
2
C
D
Coastal evolution
Time
MIS 5a?
MIS 3c*
MIS 3a*